

Stereotaxy-Based Regional Brain Volumetry Applied to Segmented MRI: Validation and Results in Deficit and Nondeficit Schizophrenia

Mario Quarantelli,* Michele Larobina,* Umberto Volpe,† Giovanni Amati,† Enrico Tedeschi,*
Andrea Ciarmiello,‡ Arturo Brunetti,* Silvana Galderisi,† and Bruno Alfano*

*Biostructure and Bioimaging Institute, National Council for Research–University “Federico II,” Via Pansini, 5, 80131 Naples, Italy;

†Department of Psychiatry, University of Naples, SUN Largo Madonna delle Grazie I, 80138 Naples, Italy; and ‡Nuclear Medicine,

IRCCS “Fondazione G. Pascale,” Via Cappella Cangiani, 80131 Naples, Italy

Received October 16, 2001

A method for postprocessing of segmented routine brain MRI studies providing automated definition of major structures (frontal, parietal, occipital, and temporal lobes; cerebellar hemispheres; and lateral ventricles) according to the Talairach atlas is presented. The method was applied to MRI studies from 25 normal subjects (NV), 14 patients with deficit schizophrenia (DS), and 14 with nondeficit schizophrenia (NDS), to evaluate their gray matter and CSF regional volumes. The two patient groups did not differ in mean age at illness onset, duration of illness, severity of psychotic symptoms, or disorganization; DS had more severe avolition and worse social functioning than NDS. For validation purposes, brain structures were manually outlined on original MR images in 10 studies, thus obtaining reference measures. Manual and automated measures were repeated 1 month apart to measure reproducibilities of both methods. The automated method required less than 1 min/operator per study vs more than 30 min for manual assessment. Mean absolute difference per structure between the two techniques was 4.8 ml. Overall reproducibility did not significantly differ between the two methods. In subjects with schizophrenia, a significant decrease in GM and increase in CSF were found. GM loss was confined to frontal and temporal lobes. Lateral ventricles were significantly larger bilaterally in NDS compared to NV and only on the right in NDS compared to DS. The finding of greater structural brain abnormalities in NDS adds to the evidence that deficit schizophrenia does not represent just the more severe end of the schizophrenia continuum. © 2002 Elsevier Science (USA)

INTRODUCTION

Segmentation of MR brain images provides measures of total brain tissue volumes. Definition of brain lobe limits in individual MR studies, coupled with brain segmentation, can provide regional brain volum-

etry, which is gaining increasing interest in the study of structural brain changes in a number of pathologies.

Differences between normal subjects and patients with schizophrenia (SC) have been demonstrated for both total intracranial gray matter (GM) (Zipursky, 1992; Harvey, 1992, 1993; Lim, 1996) and brain lobes and ventricles (Andreasen, 1986; Shenton, 1991; Buchanan, 1993; Wright, 1995, 1999; Nair, 1997; Lawrie, 1998; Saeed, 1998; Puri, 1999, 2001; Paillere-Martinot, 2001; Lieberman, 2001). However, it has been argued that schizophrenia is a heterogeneous disease, with variable clinical manifestations, probably reflecting a multiplicity of etiopathogenetic mechanisms (Maj, 1998; Tsuang *et al.*, 2000), which might be associated with different morphometric brain features. The concept of “deficit schizophrenia” (Carpenter, 1988) was introduced to identify a relatively homogeneous subgroup of patients with the diagnosis of schizophrenia, characterized by the highly stable (Amador, 1999) presence of primary negative symptoms including restricted affect, diminished emotional range, poverty of speech, curbing of interests, and reduction of sense of purpose and of social drive. Deficit patients (DS) present a poor premorbid adjustment, an often insidious onset, and a relatively high frequency of soft neurological signs, abnormal involuntary movements, and resistance to treatment with antipsychotic drugs (including atypical antipsychotics) (Buchanan, 1990; Carpenter, 1994; Fenton, 1994).

Structural brain imaging studies investigating correlates of the negative symptoms on the whole have reported abnormalities of ventricular and periventricular structures and hemispheric asymmetries (Pearlson *et al.*, 1984; Williams *et al.*, 1985; Kemali *et al.*, 1987; Van Kammen *et al.*, 1988; Bilder, 1994; Gur *et al.*, 1994; Meisenzahl, 2000), as well as of frontal lobes (Besson *et al.*, 1987; Uematsu, 1989; Williamson *et al.*, 1991; Zipursky *et al.*, 1992; Wible *et al.*, 1995). The few available studies comparing DS and nondeficit patients (NDS) have reported conflicting results (Buchanan,

1993; Turetsky, 1995). Most of these studies were carried out by manual definition of brain structures on image sets. Manual methods for definition of brain structures are cumbersome and prone to operator-dependent inaccuracy. Furthermore, the definition of brain lobe limits is particularly difficult to perform on sets of axial slices, when a 3D set of images specifically acquired for morphometric analysis is not available; this is the case when routine clinical studies are evaluated, for which an automated procedure could represent a valuable tool to decrease intra- and inter-operator variability and to save operator time. An alternative approach to brain structure definition is offered by stereotactic methods, which are based on the assumption of proportionality of brain structures (i.e., brain size changes between different subjects, but proportions of brain structures are constant). Stereotactic proportional grids were originally developed in the 1950s for stereo-EEG evaluation of temporal lobe epilepsy. Talairach introduced the line passing through the center of the anterior and posterior cerebral commissures (AC-PC) as a stable basis for the stereotactic grid placement compared to other brain structures (Talairach, 1952). This method has been subsequently extensively validated for indirect cerebral cortical localization (Steinmetz, 1989).

The Talairach stereotactic coordinate system (Talairach, 1988) is currently widely used, although with minor modifications, for intersubject normalization and for cortical localization of activation areas in nuclear medicine and MR functional studies (Friston, 1995). The Talairach proportional 3D grid provides a coordinate system for automated identification of anatomical structures, which divides the brain into 1056 boxes. Based on the original Talairach atlas, these boxes can be assigned to specific brain lobes. Consequently, the application of the grid to a single brain will divide it into lobes. The Talairach grid has been applied to 3D MR image sets specifically acquired for segmentation and volumetry purposes to obtain, from the corresponding segmented images, estimates of brain lobe volumes (Andreasen, 1996) or of smaller structures corresponding approximately to Brodmann's areas, subsequently pooled using multivariate analysis (Wright, 1999).

The method presented here follows this general approach, modified to process data obtained within routine clinical protocols and extended to measure, in addition to brain lobes, volumes of lateral ventricles.

The aims of our study were:

- to develop a method for the automated measurement of volumes of brain structures (i.e., cerebral lobes, cerebellar hemispheres, and lateral ventricles) based on the application of the stereotactic Talairach 3D proportional grid to segmented conventional SE axial MR images obtained within routine clinical protocols;

- to validate the method against manual tracing of brain structures as gold standard;
- to evaluate the reproducibility of both manual and automated techniques; and
- to apply the method to the study of brain regional volumetry to derive information on differences in brain tissues between schizophrenic and normal subjects, as well as between different subgroups (DS and NDS) of schizophrenic patients.

METHODS AND MATERIALS

Subjects

Twenty-eight patients, 14 with a diagnosis of DS (13 males, 1 female, age range 20–51) and 14 age- and sex-matched patients with a diagnosis of NDS (13 males, 1 female, age range 19–54) were studied. Inclusion criteria were the following:

- a DSM-IV diagnosis of schizophrenia, confirmed by the *Structured Clinical Interview for DSM-IV (SCID-I)* (First, 1997);
- no history of mental retardation, alcoholism, drug abuse, head injury, or electroconvulsive therapy; and
- willingness to participate in the study procedures.

DS diagnosis was established by administering the Schedule for the Deficit Syndrome (Kirkpatrick, 1989); information on the presence and stability of the negative symptomatology was gathered from at least one close relative of the patient.

Twenty-five age- and sex-matched normal volunteers (NV) were also recruited (19 males, 6 females, age range 18–50).

In all enrolled patients psychopathological evaluation was carried out by means of the expanded Brief Psychiatric Rating Scale, version 4.0 (EBPRS; Ventura *et al.*, 1993), the Scale for the Assessment of Negative Symptoms (SANS; Andreasen, 1981), and the Scale for the Assessment of Positive Symptoms (SAPS; Andreasen, 1984). The recent history of hospitalization and social functioning was also evaluated by the Strauss–Carpenter Scale (Strauss and Carpenter, 1972).

MR Studies

Analyzed brain MRI sets included T1w (600/15 TR/TE) and DP/T2w (2200/15–90 TR/TE1–TE2) conventional spin-echo images, 25-cm FOV, 256 × 256 acquisition matrix, 30 contiguous 4-mm-thick axial slices, covering the entire brain.

A subset of 10 studies (5 schizophrenic and 5 normal subjects) was used for comparison of volume measures between manual and automated techniques and for reproducibility assessment purposes. A larger data base of 50 normal subject MRI studies (age range 16–76, 31 males, 19 females) was used to define age-re-

lated total GM and CSF changes, which were used for adjustment of age-related changes in volumes here presented.

Segmentation

Segmentation of MR brain images into GM, white matter (WM), and CSF was obtained using a fully automated multispectral segmentation method (Alfano, 1997, 1998). This method provides, starting from a set of axial T1w-, T2w-, and N(H)-weighted conventional spin-echo images, a corresponding set of segmented images. The only constraint required by the algorithm is that a triplet of images (T1w, N(H), and T2w) is available for each level. Care was thus taken to ensure the same positioning for T1w and N(H)/T2w image sets in each study. Segmentation was performed binarily, i.e., each intracranial pixel was labeled as belonging univocally to GM, WM, or CSF.

Preliminary Assignment of Talairach Boxes

The Talairach 3D grid divides a box encompassing the brain into 1056 small boxes. In order to obtain structure measures from the application of the Talairach 3D grid to segmented MR images, a look-up table for the assignment of the content of each box to a specific brain structure must be used. This was done preliminarily by visual inspection of the Talairach atlas: two neuroradiologists (M.Q. and E.T.) assigned each of the 1056 boxes of the Talairach atlas to six couples of structures (frontal, parietal, occipital, and temporal lobes; cerebellar hemispheres, and lateral ventricles). Assignment was done on the original atlas (Talairach, 1988), based on the labeling of cortical structures therein reported. Boxes containing more than a structure were assigned to the one occupying their largest percentage.

Software

A program was written for application of the Talairach three-dimensional proportional grid to brain MR data sets, which performs the following steps:

I. Identification of the AC and PC

The program prompts the operator to identify the center of the AC and PC on the original axial images. This is the only operator intervention required by the method. The program also automatically provides a lateral view of the brain with display of the AC-PC line, to allow one to recognize possible major errors in commissures' identification, which results in a clearly abnormal position of such line.

II. GM Isolation

The application of the Talairach 3D grid needs identification of the external brain parenchyma limits, which

can be automatically defined on segmented images using GM voxels. Therefore, from a set of segmented axial images, a set of GM maps is automatically obtained by zeroing of all non-GM voxels. This allows one to handle the data set more efficiently, thus decreasing computational time of subsequent processing steps.

III. Generation of the GM Volume

The 30 MR axial GM maps are stacked to obtain a $256 \times 256 \times 30$ 3D matrix, which is in turn rebinned into a matrix with 1-mm isotropic voxel dimensions.

IV. Realignment of the Segmented GM Volume to the AC-PC Line

The program rotates the GM volume around the z and x axes to render the AC-PC line defined by the operator's identification in step (I) horizontal.

V. Automated Identification of the Falx Cerebri (FC)

Residual head tilt around the y axis can be corrected if the midline structures are aligned to the AC-PC line. In order to do this the FC can be used as a landmark of the midsagittal plane. In order to identify the FC, a 5-pixel-thick line is selected on the projection of the GM volume onto the coronal plane, lying at 1/6 of the distance between the AC-PC line and the top of the brain. The highest second derivative of this line, corresponding to the center of the FC, is automatically identified (Fig. 1A).

VI. Correction of Possible Rotation around the y Axis (Due to Malpositioning of the Head at the Time of the MR Scan)

Correction of head tilt around the y axis is achieved by rotating the GM brain volume so that the FC and the AC-PC line are vertically aligned (Fig. 1B).

VII. Identification of the Boundaries of a Box Encompassing the Supratentorial Brain (Fig. 2)

The limits of the GM volume are automatically identified. In order to exclude cerebellum, which is not used in the definition of the whole brain box according to Talairach, the inferior brain limit is identified as the lowermost plane containing GM in front of the AC, thus allowing automated identification of the inferior limit of the temporal tips.

VIII. Application of the Talairach Proportional Grid to the Segmented Image Set

The segmented images are then divided into 1056 small boxes according to Talairach grid prescriptions. Brain parenchyma pixels falling below the brain box are assigned to two (left and right) additional boxes, which are assigned to cerebellum.

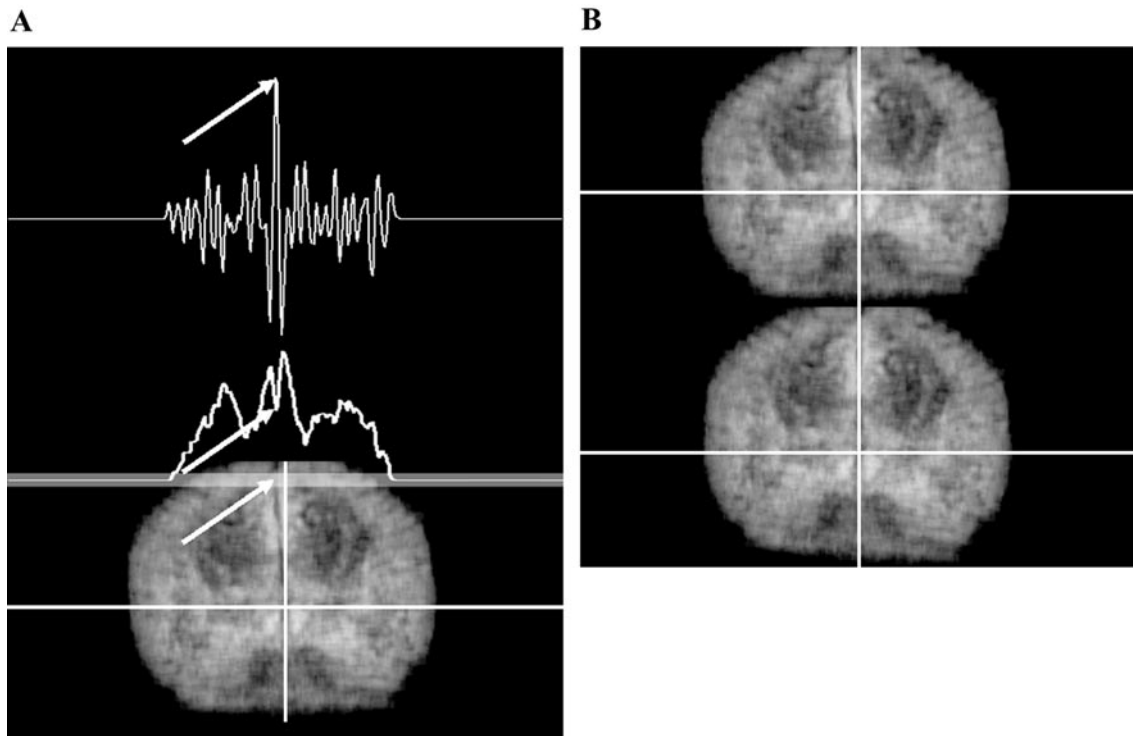


FIG. 1. (A) Projection of the GM volume onto the coronal plane after realignment to the AC-PC line (perpendicular to this plane). A 5-pixel-thick line placed at 1/6 of the distance between the AC-PC line and the brain vertex is selected (shaded area). The corresponding intensity profile is obtained (middle line). Corresponding second derivative is then calculated (upper line); its highest value identifies the superior sagittal sinus (arrows). (B) The rotation angle needed to vertically align the superior sagittal sinus and the AC-PC line (upper image) is then applied to the GM volume, thus correcting for malrotation around the y axis.

IX. Sum of the Boxes Belonging to Each of the 12 Structures

For each lobe and for each cerebellar hemisphere, GM contained in the corresponding boxes, according to the lookup table preliminarily created, is summed together. The same procedure is applied to CSF voxels from the boxes containing the lateral ventricles.

X. Volume Calculation

Finally, conversion into milliliters of tissue is obtained by multiplying the pixel volume by the number of tissue pixels belonging to each structure.

Brain Structure Manual Definition (Gold Standard)

For comparison purposes, manual definition of brain lobes, cerebellar hemisphere, and lateral ventricle limits was performed on the original axial images of 10 studies by two neuroradiologists (M.Q. and E.T.).

Brain Lobes Automated Definition

On each study two neuroradiologists (M.Q. and E.T.) and two properly trained psychiatry residents (U.V. and G.A.) defined the location of the cerebral commissures for Talairach grid application.

All the software for manual and automated definition of brain structures was written using Interactive Data Language (Research Systems, Inc., Boulder, CO). Software development and data processing were performed on a Pentium-based PC (Compaq Computer Corp., U.S.A.) running Linux RedHat 7.0 and on an Ultra-Sparc 70 (Sun Microsystems, Inc., Palo Alto, CA) running Solaris 5.7.

Data Normalization

For each study, total GM, WM, and CSF were divided by total intracranial volume (ICV), thus providing fractional results (fGM, fWM, and fCSF). fGM and fCSF were corrected according to age-related changes by adjusting them to the mean age of all 56 studies (34.8 years), according to the corresponding rates of decline (for fGM, $0.013\% \cdot y^{-1}$) or of increase (for fCSF, $0.015\% \cdot y^{-1}$), as measured in a larger data base of 50 normal subjects (Alfano, 1997). Regional fGM and fCSF data were also proportionally corrected.

Automated Method Validation

Volume Measurement Comparison

As systematic differences in brain shape between diagnostic categories may theoretically induce system-

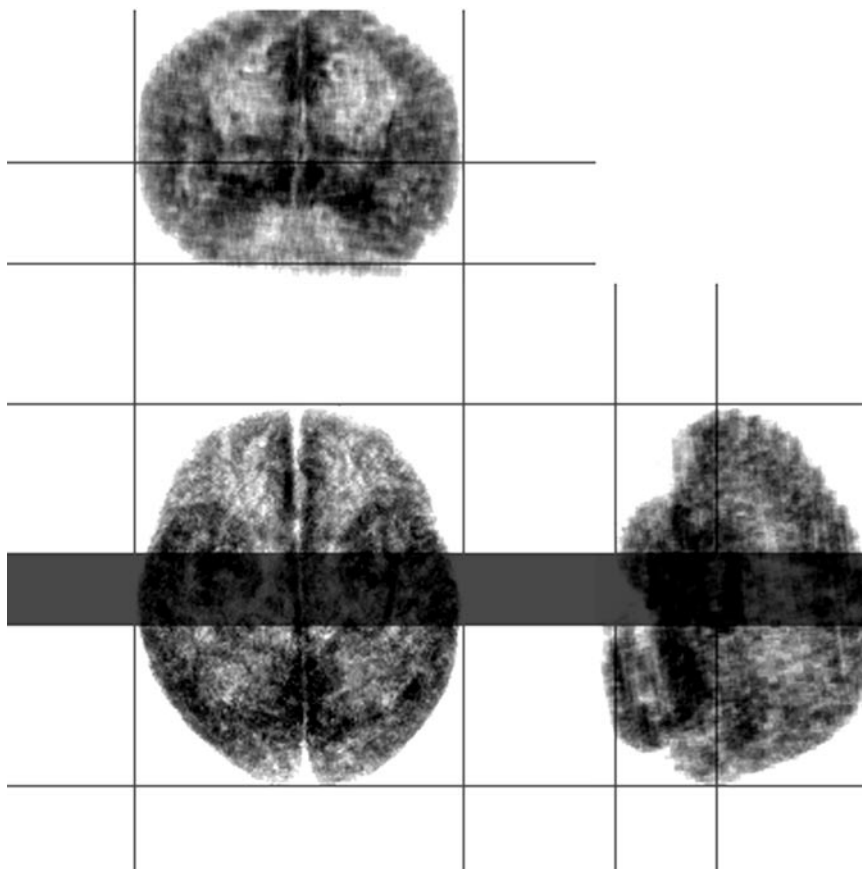


FIG. 2. Projection of the gray matter volume, realigned according to Talairach, onto the coronal (top), sagittal (bottom right), and axial (bottom left) planes. The limits of the box encompassing the brain and the AC-PC line are also displayed. The volume between the two coronal planes passing through the commissures is shaded. Note that the inferior limit of the box encompassing the brain is tangent to the inferior limit of the temporal tips, as prescribed by Talairach's 3D grid, not taking into account cerebellum. Voxels falling below this plane are automatically assigned to the cerebellum by the program.

atic errors when measuring regional volumes against a constant atlas, consistency of the agreement between the automated and the manual methods was preliminarily tested by comparing for each structure mean percentage differences between the two methods in the two main diagnostic categories (NV vs SC) by Student's paired *t* test.

Upon verification of the absence of a diagnostic category effect, data from the five NV and five SC studies analyzed with both methods were pooled for subsequent analysis, and lobar and ventricular volumes obtained using the two methods were compared using intraclass correlation coefficients (ICC) (McGraw, 1996). The disagreement between the two methods was assessed according to Bland and Altman (1986).

Localization Accuracy

When measuring the volume of a brain structure in a single study, manual and automated methods can provide the same volume estimates. This does not imply that the same voxels have been assigned to a specific structure

by both methods, it just means that the same number of voxels has been assigned to that structure.

The accuracy of "localization" of the brain structures of the automated method (i.e., the ability to correctly classify each voxel as belonging to the corresponding brain structure as defined by the gold standard, hereinafter referred to as "sensitivity") was assessed using the manual method as gold standard. Specificity of the method (measured by the voxels incorrectly classified, hereinafter defined "localization error") was also assessed compared to the manual method. For each structure, sensitivity and localization error of the automated method were calculated as the percentage of GM (for brain lobes and cerebellar hemispheres) and CSF (for lateral ventricles) voxels which were respectively correctly and incorrectly classified by the automated technique in the 10 MR studies analyzed by both methods (manual and automated) in two separate measures.

For each structure, sensitivity is expressed as percentage of the volume as measured by the manual

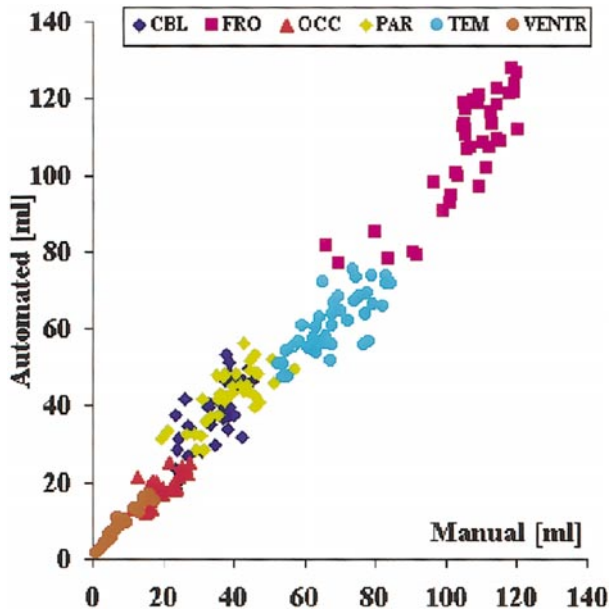


FIG. 3. Manual vs automated measurements of brain structure volumes. Data are reported for the two measures of the 12 structures performed with each method on the 10 MR studies used for validation ($n = 240$). For each structure, right and left data are represented in the same color. CBL, cerebellum; FRO, frontal; OCC, occipital; TEM, temporal; PAR, parietal; VENTR, lateral ventricles.

technique and localization error as percentage of the volume as measured by the automated technique.

Reproducibility

The same 10 studies used for lobar reproducibility assessment were analyzed twice 1 month apart with both manual and semiautomated techniques to assess intraoperator reproducibility of the two techniques. Reproducibilities of the two techniques were compared using Student's paired t test.

Group Comparisons

Age-corrected (for fGM and fCSF) regional data, resulting from the application of the automated method to the 25 NV and 28 SC studies, were compared using t test: first, differences were sought between NV and pooled SC data, and only for regions showing differences between these two groups, differences of NV vs DS, NV vs NDS, and DS vs NDS were then probed separately. Demographic and clinical characteristics of the different groups were compared using the t test.

Results were considered significant when $P < 0.05$. Where necessary, multiple comparison correction according to Bonferroni was applied.

RESULTS

For each study, operator intervention required less than 1 min for the definition of the AC-PC line. Manual

definition of brain lobes required on average 37 min (range 30–48) for each study. Volumes obtained by manual assessment vs corresponding automated measures are plotted in Fig. 3.

Automated Method Validation

Volume Measurement Comparison

In Table 1, mean differences between the two methods, separately for NV and SC studies, are reported for each structure. Comparison of the agreement between the two methods in NV and SC failed to demonstrate a difference in accuracy of the automated method upon the two diagnostic categories, hence for subsequent validation of the automated method NV and SC data were pooled.

The results of the comparison of the lobar volumes as measured by the two techniques, after pooling the results from five NV and five SC studies used for method comparison, are reported in Table 2 along with corresponding ICC.

The differences between the two methods are plotted in Fig. 4 according to Bland and Altman (1986). The mean difference between automated and manual mea-

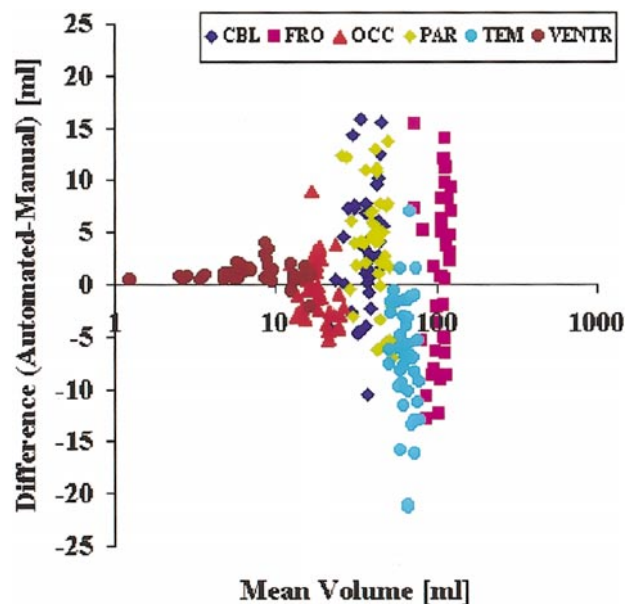


FIG. 4. Scatter plot of the differences between automated and manual measures of the volumes of the 12 structures (y axis, linear scale) versus the average values obtained from the two methods (x axis, logarithmic scale) according to Bland and Altman (1986). A positive value indicates overestimate by the automated method. Data from the two measures of 12 brain structures performed with each method in 10 MR studies are reported (for each structure, $n = 240$). Symbols are the same as in Fig. 3. Mean absolute difference between the values obtained by the two techniques was 4.8 ml, maximum difference for a single structure was 21.4 ml. Overestimation by the automated method is present for ventricles, cerebellum, and parietal lobes, underestimation is present for temporal lobes, with increased error for larger structures.

TABLE 1

Differences between Automated and Manual Methods Expressed as Percentage of the Volume Measured Manually Separately in NV and SC Studies

	% difference ($n = 20$)	
	NV mean \pm SD	SC mean \pm SD
Cerebellum	5.8 \pm 13.4	13.6 \pm 23.9
Frontal	4.2 \pm 7.4	-0.8 \pm 8.2
Occipital	-1.8 \pm 14.2	0.1 \pm 21.6
Parietal	10.9 \pm 13.9	12.9 \pm 20.9
Temporal	-11.6 \pm 6.4	-7.3 \pm 9.0
Lat. ventricles	24.7 \pm 16.2	23.7 \pm 17.7

Note. For each lobe and for each group of subjects (NV and SC) are reported the average of 20 measures (right and left, 5 MR studies analyzed twice) performed with each method. No significant difference in the performance of the automated method when analyzing NV and SC was detected by testing % differences by Student's paired t test. SD, standard deviation.

sure of each structure in the 10 MR studies was 0.4 ml (range -6.8 to 3.7), the maximum difference for a single measure being 21.4 ml. The values for the single structures along with the corresponding values for absolute differences are reported in Table 2. Overestimation by the automated method for ventricles, cerebellum, and parietal lobes and underestimation for temporal lobes were statistically significant at paired t test. For lateral ventricles, volume overestimation by the automated method (+1.1 ml) corresponds to a 13% error. For the remaining GM structures (cerebellar hemispheres and brain lobes), systematic errors were within 10%.

TABLE 2

Comparison of the Brain Lobe Volumes Obtained Using Manual Assessment vs Those Obtained Using the Automated Method ($n = 40$)

	Manual (ml) mean \pm SD	Automated (ml) mean \pm SD	Signed difference (ml) mean \pm SD	Absolute difference (ml) mean \pm SD	ICC	Sensitivity	Localization error
Cerebellum ^a	34.4 \pm 6.4	37.5 \pm 8.3	3.1 \pm 5.9	5.2 \pm 4.2	0.7744	89.5%	19.5%
Frontal	105.2 \pm 17.9	106.8 \pm 19.4	1.6 \pm 7.9	7.0 \pm 3.9	0.9082	88.2%	13.3%
Occipital	19.1 \pm 4.2	18.5 \pm 3.4	-0.5 \pm 3.1	2.6 \pm 1.7	0.7206	86.0%	10.9%
Parietal ^a	39.4 \pm 8.6	43.1 \pm 7.0	3.7 \pm 5.6	5.7 \pm 3.6	0.8068	78.8%	30.6%
Temporal ^a	68.4 \pm 9.0	61.7 \pm 7.7	-6.8 \pm 6.0	7.3 \pm 5.4	0.8042	86.8%	3.4%
Lat. ventricles ^a	7.4 \pm 4.6	8.5 \pm 4.5	1.2 \pm 1.0	1.2 \pm 0.8	0.9904	96.7%	18.2%
Mean			0.4 \pm 6.4	4.8 \pm 4.2	0.9909	88.3%	11.7%

Note. Mean and standard deviation (SD) are reported for both signed (automated minus manual) and absolute differences between the two methods. For each structure, the percentages of voxels correctly and incorrectly assigned by the automated method (respectively, sensitivity and localization inaccuracy of the automated method, average of the two trials in 10 studies), are reported in the last two columns. For each structure, sensitivity is expressed as a percentage of the volume as measured by the manual technique, localization error as a percentage of the volume as measured by the automated technique, while mean sensitivity and localization error are calculated over total brain voxels. For each lobe, the averages of 40 measures (right and left, 10 MR studies analyzed twice) performed with each method are reported. SD, standard deviation. Correlation as assessed by intraclass correlation coefficients (ICC) was significant in all instances.

^a Mean volumes, as measured with manual and automated methods, significantly different at paired t test.

Localization Accuracy

Sensitivity and specificity assessment results are reported in the last two columns of Table 2. Two representative studies are reported in Fig. 5. The voxels incorrectly labeled by the automated method are highlighted. The selected studies are the two associated with the worst (Fig. 5A, mean error per structure 11.2 ml) and the best (Fig. 5B, mean error per structure 3 ml) performances of the automated method.

Reproducibility

The results of the assessment of the reproducibility of the two techniques are summarized in Table 3. The automated method was significantly less reproducible for cerebellar hemispheres, while manual measures were less reproducible than the automated method for temporal lobes. When pooling all structures, no differences in the reproducibilities of the two techniques could be detected.

Group Comparisons

There was no significant difference between DS and NDS for age (37.1 \pm 8.4 vs 34.8 \pm 8.5 years), education (11.2 \pm 2.9 vs 11.3 \pm 3.8 years of school), age at onset of illness (22.1 \pm 4.82 vs 19.5 \pm 4.2 years), or duration of illness (15.1 \pm 8.7 vs 15.3 \pm 6.6 years). The mean current dose of antipsychotic drugs was higher in NDS patients (608 \pm 209 vs 425 \pm 336 chlorpromazine equivalents). There was no difference between the two patient groups as to the type of antipsychotic treatment they were receiving: 54.5% of DS and 53.8% of NDS patients were being treated with novel antipsychotics, 27.3% vs 30.8% with standard neuroleptics,

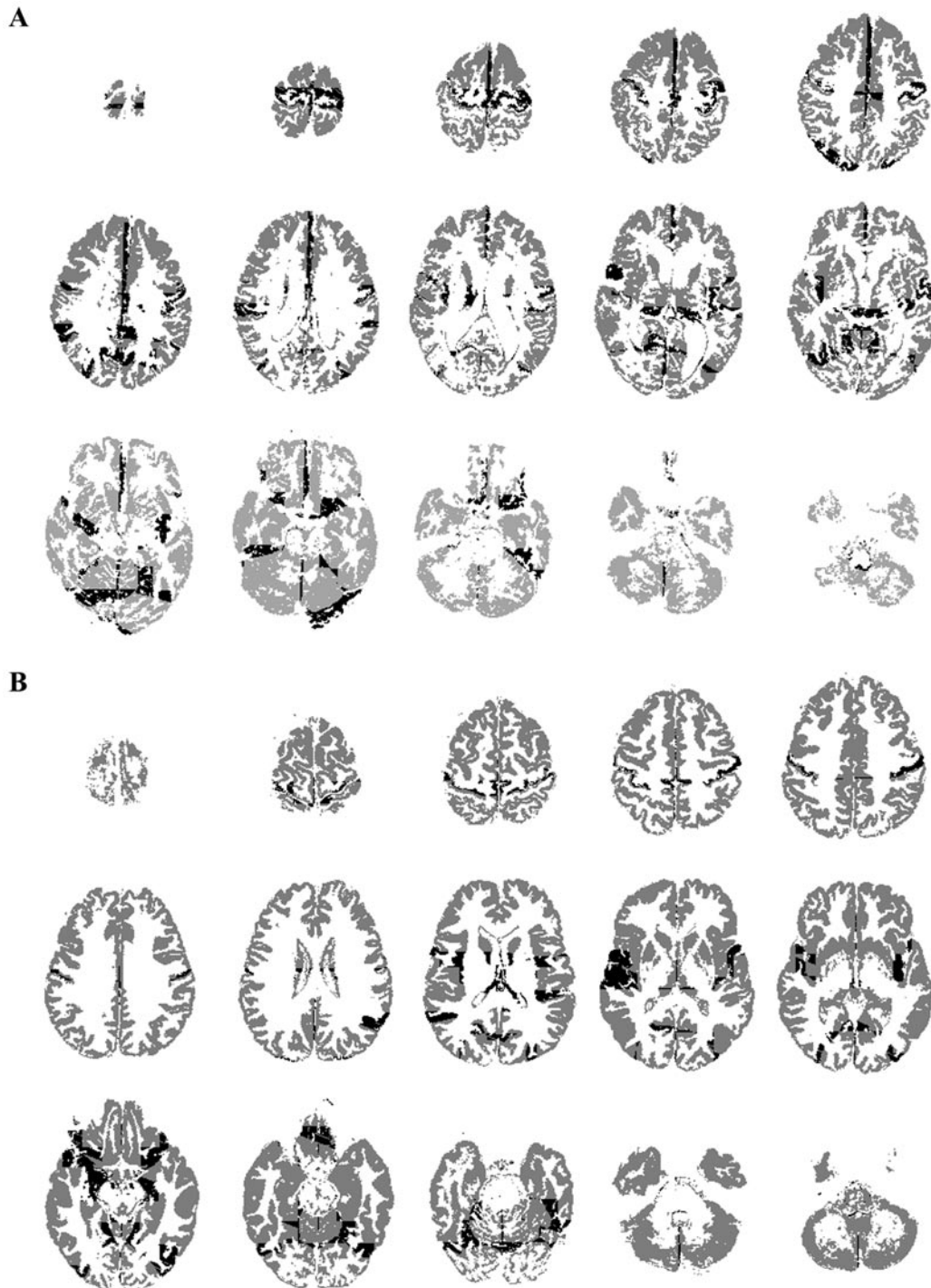


FIG. 5. Representative slices from the two segmented MRI studies with the largest (study A, mean error per structure 11.2 ml) and the smallest (study B, mean error per structure 3 ml) error. For sake of simplicity only GM is represented. GM voxels correctly assigned by the automated method are in gray, incorrectly assigned voxels are in black.

18.2% vs 15.4% with a combination of standard and novel antipsychotics.

The mean score on the Avolition–Apathy SANS subscale was significantly higher in DS than in NDS patients (DS, 3.71 ± 0.7 ; NDS, 2.85 ± 0.9 ; $t = 2.68$, $P <$

0.01). No significant difference was found on SAPS and EBPRS scores. On the Strauss–Carpenter Scale, DS patients, compared to NDS, had significantly lower total score (DS, 7.2 ± 2.3 ; NDS, 10.0 ± 2.6 ; $t = -2.90$, $P < 0.008$) and mean score for the item Social Contacts

TABLE 3Mean Absolute Intramethod Differences for Manual and Automated Methods ($n = 20$)

	Manual		Automated	
	Mean (ml)	Max (ml)	Mean (ml)	Max (ml)
CBL ^a	0.4	1.3	6.9	14.8
FRO	3.2	13.9	4.9	12.2
OCC	1.5	4.6	1.2	2.6
PAR	4.3	16.2	2.4	8.3
TEM ^a	4.8	12.9	1.9	4.4
VENTR	0.4	1.4	0.4	1.6
Total ($n = 120$)	2.4	16.2	2.9	14.8

Note. For each structure $n = 20$ (2 structures for 10 studies, as right and left structures are pooled together), mean and maximum values are reported. Units are milliliters of GM (brain lobes and cerebellar hemispheres) or of CSF (lateral ventricles). Reproducibility of the manual method was significantly higher at paired t test for cerebellar hemispheres and significantly lower for the temporal lobes. When all structures were pooled together, no differences in the reproducibilities of the two methods emerged.

^a Difference in reproducibilities significant at paired t test after correction for multiple comparisons.

(DS, 0.7 ± 1.0 ; NDS, 2.5 ± 1.5 ; $t = -3.59$, $P < 0.002$), indicating poorer functioning in the former group.

Calculation of total intracranial GM, WM, and CSF fractional volumes showed a significant decrease in fGM, with a corresponding increase in CSF, in patients compared to NV (Fig. 6). This was common to both subtypes of SC, with a more evident, although not significant, effect in NDS patients (Fig. 7). No significant difference was present for fGM and fCSF between DS and NDS.

Results of the regional volumes assessment in the three groups of subjects are summarized in Table 4. The reduction in fGM appears to be essentially due to a decrease in frontal and temporal lobe GM volumes. Again, no difference emerges between the two SC subgroups.

Enlargement of lateral ventricles was present in the SC population; for the right ventricle, it was significant in NDS versus both NV and DS, while for the left ventricle, it was significant in NDS versus NV, but approached significance only versus DS.

DISCUSSION

Validation of the automated method implied a comparison between two methods for definition of major brain structures, which are based on two intrinsically different approaches, such as a landmark-based (manual definition of structures is based on the recognition of internal landmarks) and a proportionality-based (stereotaxy-based) method. Nonetheless, in agreement with previous work validating this approach on 3D

data sets (Andreasen, 1996), the differences between the two methods, although systematic for most structures, fall within 10% for GM volumes and below 15% for ventricular volumes, largely within the reproducibility interval of both techniques. In this work manual assessment of brain structures, operated on axial slices by two experienced neuroradiologists, had the same overall reproducibility compared to the automated technique despite the substantial amount of time spent in the manual process.

The inferior reproducibility of the automated method when measuring the cerebellar hemispheres, compared to manual assessment, is a somewhat expected finding, considering that the extremely well defined boundaries of the cerebellum do not allow for interoperator variability, while the stereotactic proportional approach makes the volume of this structure extremely dependent on the height at which the AC-PC line is defined. In this sense the lower reproducibility of the manual technique when measuring the temporal lobe is also expected, as the upper part of this region has less well defined boundaries, hard to univocally define especially on axial slices.

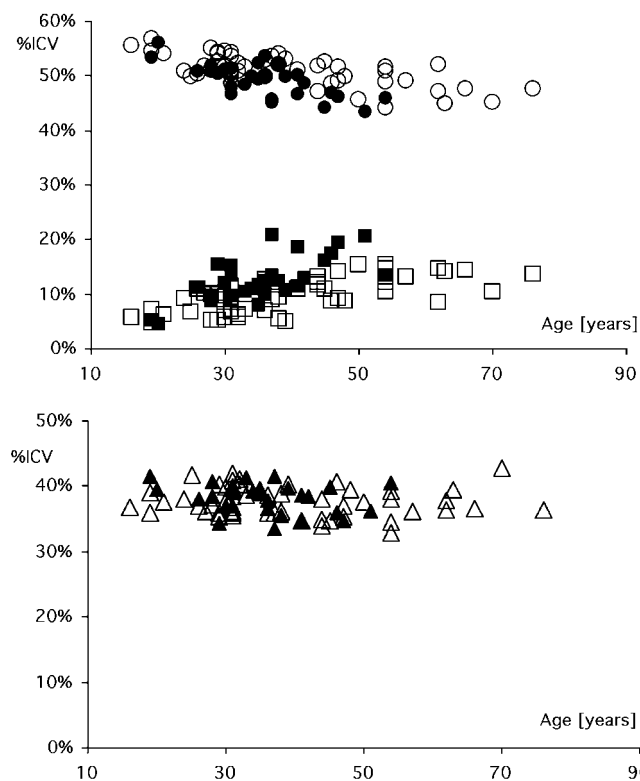


FIG. 6. Scatter plots of GM (circles), WM (triangles), and CSF (squares) percentages of ICV as a function of age in 50 normal subjects (empty marks) vs 28 schizophrenic patients (solid marks). In patients a significant decrease in GM and an increase in CSF can be appreciated, with normal fractional WM volumes. Differences in fractional tissue volumes were not significant between DS and NDS patients, hence patient data are pooled.

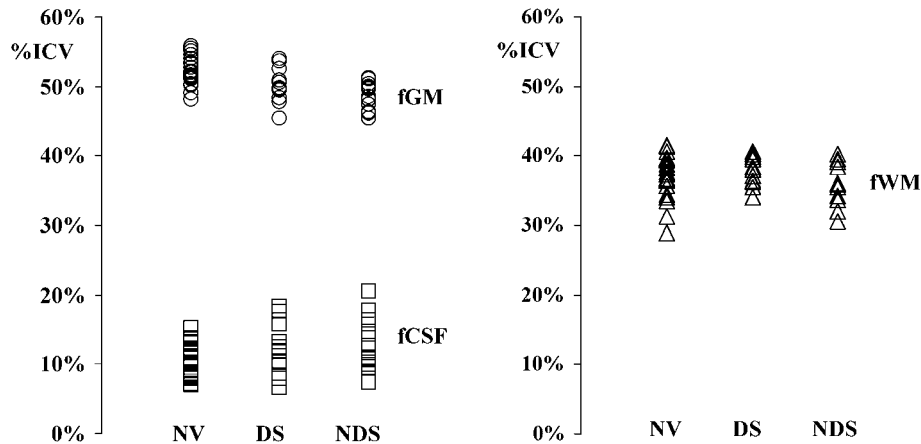


FIG. 7. Fractional GM (circles), CSF (squares), and WM (triangles) volumes in NV, DS, and NDS. Data are % of total intracranial volume, age corrected to the mean age of all subjects. In schizophrenic patients, fGM is significantly lower and fCSF significantly higher than in normal subjects. No significant difference was found between deficit and nondeficit schizophrenic patients.

An advantage of this type of approach to regional definition consists in its modularity. Once the brain has been divided into boxes, they can be assembled to measure different structures depending on what specific anatomic structure is being studied or even assembled according to the patterns of their modifications, as proposed by others (Wright, 1999).

Regional volumetry through the subdivision in boxes of the brain operated by the Talairach 3D grid allows only an identification of major divisions of the brain, where the resolution limit is given by the size of the subdivisions operated by the grid, hence not allowing one to measure the size of small brain structures (e.g., basal ganglia or amygdala).

To overcome these limitations, a voxel-wise approach to comparison of local concentration of gray matter between groups of subjects has been recently published (Ashburner, 2000). The procedure involves spatial registration into the stereotactic space of the MRI volumes; subsequent segmentation into GM, WM, and CSF; smoothing of GM volumes; and finally voxel-wise parametric statistical testing to compare GM distribution. Corrections for multiple comparisons, of major impact in voxel-based comparisons, are made according to the Worsley approach to Gaussian random fields.

A critical problem with the voxel-wise approach, however, appears to be the registration step, because registration errors result in apparent strong interstudy

TABLE 4

Fractional Volumes of All Structures in the Three Groups

	Ventricle		Cerebellum		Frontal		Temporal		Occipital		Parietal	
	Mean	SD	Mean	SD	Mean	SD	Mean	SD	Mean	SD	Mean	SD
Right												
NV	0.4% ^{a,b}	0.2%	3.0%	0.6%	10.4% ^{a,b,c}	0.7%	6.9% ^{a,b,c}	0.4%	1.9%	0.3%	4.0%	0.4%
DS	0.5% ^d	0.2%	3.0%	0.7%	10.1%	0.7%	6.7%	0.5%	1.9%	0.2%	4.0%	0.4%
NDS	0.8%	0.3%	2.7%	0.5%	9.8%	0.6%	6.3%	0.5%	1.6%	0.3%	3.9%	0.4%
Left												
NV	0.5% ^{a,b}	0.2%	3.3%	0.7%	9.7% ^{a,b,c}	0.6%	7.1% ^{a,b,c}	0.4%	2.0%	0.3%	4.0%	0.4%
DS	0.5%	0.2%	3.2%	0.7%	9.5%	0.7%	6.8%	0.5%	2.0%	0.3%	3.9%	0.5%
NDS	0.9%	0.4%	2.9%	0.5%	9.1%	0.7%	6.5%	0.4%	1.8%	0.3%	4.0%	0.4%

Note. Values are means and standard deviations (SD) of age-corrected GM (for brain lobes and cerebellar hemispheres) and CSF fractions of ICV. The decrease in GM, with corresponding increase in CSF, appears mainly localized at the level of frontal and temporal lobes bilaterally in both groups of patients. Right lateral ventricle is significantly increased in size in NDS compared to both the NV and the DS groups. Left lateral ventricle shows the same trend, but the difference between the two patient groups only approaches significance.

^a NV and pooled schizophrenic patients significantly different.

^b NV and NDS patients significantly different.

^c NV and DS patients significantly different.

^d DS and NDS schizophrenic patients significantly different.

differences in GM distribution. This is decreased only to a limited extent by smoothing, leaving residual effects in areas of strong image gradients, which also make this approach unfeasible when 3D data sets, with fine brain sampling, are not available. At the present stage voxel-based methods, although apparently increasing the detail of the differences that can be appreciated, provide data that must be critically examined, as they are prone to false positive results that can be avoided only when large regions are averaged.

Also when morphometry is not a focus, the vast majority of clinical trials on SC include MRI in the protocol, which is indeed a necessary tool in the workup of SC.

The presented method is independent of original data set type and segmentation method. In the present implementation it has been applied to 30 4-mm-thick contiguous slices, but in theory it can be applied to even smaller data sets, further undersampling the brain, as long as voxel dimensions remain below the order of magnitude of the grid boxes and the whole brain is covered. The method is thus suitable to analyze virtually any standard MRI data set following segmentation, providing a tool to obtain regional volume data that otherwise would not be taken advantage of.

Regarding possible application of the automated method in the study of other types of pathologic conditions, it must be stressed that, due to the underlying assumption of proportionality and symmetry of the brain structures, the use of a stereotactic approach does not apply in all cases. It is not suitable, for example, when normal anatomy is altered for the presence of mass lesions.

Application of the method to MR images obtained from conventional SE allowed an assessment of regional volumetric changes in SC, which confirmed previous literature data regarding frontotemporal involvement in this pathology and disclosed a differential involvement of lateral ventricle in NDS and DS. We found indeed larger lateral ventricles in NDS compared to both NV and DS. Unlike others (Buchanan, 1993), we have not found a significant difference between DS and NDS concerning volumetry of frontal regions: in both patient subgroups fGM in these regions was significantly smaller compared to NV. This can be explained by the fact that we have measured the frontal lobes without assessing any specific structure, whose reduction may be diluted when considering the whole lobe.

The two patient groups did not differ in mean age at illness onset, duration of illness, severity of psychotic symptoms, or disorganization; DS had more severe avolition and worse social functioning than NDS. The finding of greater structural brain abnormalities in NDS adds to the evidence that deficit schizophrenia does not represent just the more severe end of the schizophrenia continuum and suggests different phys-

iopathological mechanisms in the two schizophrenia subtypes.

Further work is needed to enlarge the data base to confirm these initial findings and to clarify the meaning of these differences, especially in relationship to patients' history and clinical picture.

ACKNOWLEDGMENTS

Part of this work has been carried out within PVEOut, an EC-cofinanced R&TD project (5th Framework Programme, Contract QLG3-CT2000-594), and supported by Grant 9806499118-01 from the Italian Ministry of University and Scientific Research, by Regione Campania (L. 41/94), and by Ministero della Sanità (Progetto Alzheimer, Attività di ricerca finalizzata D.Lgs. 502/92 e D.Lgs. 229/99).

REFERENCES

- Alfano, B., Brunetti, A., Covelli, E. M., Quarantelli, M., Panico, M. R., Ciarmiello, A., and Salvatore, M. 1997. Unsupervised, automated segmentation of the normal brain using a multispectral relaxometric magnetic resonance approach. *Magn. Reson. Med.* **37**: 84–93.
- Alfano, B., Quarantelli, M., Brunetti, A., Larobina, M., Covelli, E. M., Tedeschi, E., and Salvatore, M. 1998. Reproducibility of intracranial volume measurement by unsupervised multispectral brain segmentation. *Magn. Reson. Med.* **39**: 497–499.
- Amador, X. A., Kirkpatrick, B., Buchanan, R. W., Carpenter, W. T., Jr., Marcinko, L., and Yale, S. A. 1999. Stability of the diagnosis of the deficit syndrome in schizophrenia. *Am. J. Psychiatry* **156**: 637–639.
- Andreasen, N., Nasrallah, H. A., Dunn, V., Olson, S. C., Grove, W. M., Ehrhardt, J. C., Coffman, J. A., and Crosssett, J. H. 1986. Structural abnormalities in the frontal system in schizophrenia. A magnetic resonance imaging study. *Arch. Gen. Psychiatry* **43**: 136–144.
- Andreasen, N. C., Rajarethinam, R., Cizadlo, T., Arndt, S., Swayze, V. W., 2nd, Flashman, L. A., O'Leary, D. S., Ehrhardt, J. C., and Yuh, W. T. 1996. Automatic atlas-based volume estimation of human brain regions from MR images. *J. Comput. Assisted Tomogr.* **20**: 98–106.
- Ashburner, J., and Friston, K. J. 2000. Voxel-based morphometry—The methods. *NeuroImage* **11**: 805–821.
- Besson, J. A., Corrigan, F. M., Cherryman, G. R., and Smith, F. W. 1987. Nuclear magnetic resonance brain imaging in chronic schizophrenia. *Br. J. Psychiatry* **150**: 161–163.
- Bilder, R. M., Wu, H., Bogerts, B., Degreaf, G., Ashtari, M., Alvir, J. M., Snyder, P. J., and Lieberman, J. A. 1994. Absence of regional hemispheric volume asymmetries in first-episode schizophrenia. *Am. J. Psychiatry* **151**: 1437–1447.
- Bland, J. M., and Altman, D. G. 1986. Statistical method for assessing agreement between two methods of clinical measurement. *Lancet* **8476**: 307–310.
- Buchanan, R. W., Breier, A., Kirkpatrick, B., Elkashef, A., Munson, R. C., Gellad, F., and Carpenter, W. T., Jr. 1993. Structural abnormalities in deficit and nondeficit schizophrenia. *Am. J. Psychiatry* **150**: 59–65.
- Buchanan, R. W., Kirkpatrick, B., Heinrichs, D. W., and Carpenter, W. T., Jr. 1990. Clinical correlates of the deficit syndrome of schizophrenia. *Am. J. Psychiatry* **147**: 290–294.
- Carpenter, W. T., Jr., Heinrichs, D. W., and Wagman, A. M. 1998. Deficit and nondeficit forms of schizophrenia: The concept. *Am. J. Psychiatry* **145**: 578–583.

- Carpenter, W. T., Jr. 1994. The deficit syndrome. *Am. J. Psychiatry* **151**: 327–329.
- Fenton, W. S., and McGlashan, T. H. 1994. Antecedents, symptom progression, and long-term outcome of the deficit syndrome in schizophrenia. *Am. J. Psychiatry* **151**: 351–356.
- First, M. B., Spitzer, R. L., Gibbon, M., and Williams, J. B. W. 1997. *Structured Clinical Interview for DSM-IV Axis I Disorders (SCID-I), Clinician Version*. Am. Psychiatric Press, Washington, DC.
- Friston, K. J., Ashburner, J., Poline, J. B., Frith, C. D., Heather, J. D., and Frackowiak, R. S. J. 1995. Spatial registration and normalization of images. *Hum. Brain Mapping* **2**: 165–189.
- Gur, R. E., Mozley, P. D., Shtasel, D. L., Cannon, T. D., Gallacher, F., Turetsky, B., Grossman, R., and Gur, R. C. 1994. Clinical subtypes of schizophrenia: Differences in brain and CSF volume. *Am. J. Psychiatry* **151**: 343–350.
- Harvey, I., Ron, M. A., DuBoulay, G., Wicks, D., Lewis, S. W., Feinstein, A., and Murray, R. M. 1995. Cortical volume reduction in schizophrenia using MRI. *Clin. Neuropharmacol.* **15**(Suppl. 1 Pt. A): 120A–121A.
- Harvey, I., Ron, M. A., Du Boulay, G., Wicks, D., Lewis, S. W., and Murray, R. M. 1993. Reduction of cortical volume in schizophrenia on magnetic resonance imaging. *Psychol. Med.* **23**: 591–604.
- Kemali, D., Maj, M., Galderisi, S., Salvati, A., Starace, F., Valente, A., and Pirozzi, R. 1987. Clinical, biological, and neuropsychological features associated with lateral ventricular enlargement in DSM-III schizophrenic disorder. *Psychiatry Res.* **21**: 137–149.
- Kirkpatrick, B., Buchanan, R. W., McKenney, P. D., Alphas, L. D., and Carpenter, W. T., Jr. 1989. The schedule for the deficit syndrome: An instrument for research in schizophrenia. *Psychiatry Res.* **30**: 119–123.
- Lawrie, S. M., and Abukmeil, S. S. 1998. Brain abnormality in schizophrenia. A systematic and quantitative review of volumetric magnetic resonance imaging studies. *Br. J. Psychiatry* **172**: 110–120.
- Lieberman, J., Chakos, M., Wu, H., Alvir, J., Hoffman, E., Robinson, D., and Bilder, R. 2001. Longitudinal study of brain morphology in first episode schizophrenia. *Biol. Psychiatry* **49**: 487–499.
- Lim, K. O., Tew, W., Kushner, M., Chow, K., Matsumoto, B., and DeLisi, L. E. 1996. Cortical gray matter volume deficit in patients with first-episode schizophrenia. *Am. J. Psychiatry* **153**: 1548–1553.
- Maj, M. 1998. Critique of the DSM-IV operational diagnostic criteria for schizophrenia. *Br. J. Psychiatry* **172**: 458–460.
- McGraw, K. O., and Wong, S. P. 1996. Forming inferences about some intraclass correlation coefficients. *Psychol. Methods* **1**: 30–46.
- Meisenzahl, E. M., Frodl, T., Zetsche, T., Leinsinger, G., Heiss, D., Maag, K., Hegerl, U., Hahn, K., and Moller, H. J. 2000. Adhesion interthalamica in male patients with schizophrenia. *Am. J. Psychiatry* **157**: 823–825.
- Nair, T. R., Christensen, J. D., Kingsbury, S. J., Kumar, N. G., Terry, W. M., and Garver, D. L. 1997. Progression of cerebroventricular enlargement and the subtyping of schizophrenia. *Psychiatry Res.* **74**: 141–150.
- Paillere-Martinot, M., Caclin, A., Artiges, E., Poline, J. B., Joliot, M., Mallet, L., Recasens, C., Attar-Levy, D., and Martinot, J. L. 2001. Cerebral gray and white matter reductions and clinical correlates in patients with early onset schizophrenia. *Schizophrenia Res.* **50**: 19–26.
- Pearlson, G. D., Garbacz, D. J., Breakey, W. R., Ahn, H. S., and DePaulo, J. R. 1984. Lateral ventricular enlargement associated with persistent unemployment and negative symptoms in both schizophrenia and bipolar disorder. *Psychiatry Res.* **12**: 1–9.
- Puri, B. K., Hutton, S. B., Saeed, N., Oatridge, A., Hajnal, J. V., Duncan, L., Chapman, M. J., Barnes, T. R., Bydder, G. M., and Joyce, E. M. 2001. A serial longitudinal quantitative MRI study of cerebral changes in first-episode schizophrenia using image segmentation and subvoxel registration. *Psychiatry Res.* **106**: 141–150.
- Puri, B. K., Richardson, A. J., Oatridge, A., Hajnal, J. V., and Saeed, N. 1999. Cerebral ventricular asymmetry in schizophrenia: A high resolution 3D magnetic resonance imaging study. *Int. J. Psychophysiol.* **34**: 207–211.
- Saeed, N., Puri, B. K., Oatridge, A., Hajnal, J. V., and Young, I. R. 1998. Two methods for semi-automated quantification of changes in ventricular volume and their use in schizophrenia. *Magn. Reson. Imaging* **16**: 1237–1247.
- Shenton, M. E., Kikinis, R., McCarley, R. W., Metcalf, D., Tieman, J., and Jolesz, F. A. 1991. Application of automated MRI volumetric measurement techniques to the ventricular system in schizophrenics and normal controls. *Schizophrenia Res.* **5**: 103–113.
- Steinmetz, H., Furst, G., and Freund, H. J. 1989. Cerebral cortical localization: Application and validation of the proportional grid system in MR imaging. *J. Comput. Assisted Tomogr.* **13**: 10–19.
- Strauss, J. S., and Carpenter, W. T. 1972. The prediction of outcome in schizophrenia. I. Characteristics of outcome. *Arch. Gen. Psychiatry* **27**: 739–746.
- Talairach, J., Ajuriaguerra, J. D., and David, M. 1952. Etudes stereotaxiques des structures encephaliques profondes chez homme. *Presse Med.* **28**: 605–609.
- Talairach, J., and Tournoux, P. 1988. *Co-planar Stereotaxic Atlas of the Human Brain*. Thieme, New York.
- Tsuang, M. T., Stone, W. S., and Faraone, S. V. 2000. Toward reformulating the diagnosis of schizophrenia. *Am. J. Psychiatry* **157**: 1041–1050.
- Turetsky, B., Cowell, P. E., Gur, R. C., Grossman, R. I., Shtasel, D. L., and Gur, R. E. 1995. Frontal and temporal lobe brain volumes in schizophrenia. Relationship to symptoms and clinical subtype. *Arch. Gen. Psychiatry* **52**: 1061–1070.
- Uematsu, M., and Kaiya, H. 1989. Midsagittal cortical pathomorphology of schizophrenia: A magnetic resonance imaging study. *Psychiatry Res.* **30**: 11–20.
- van Kammen, D. P., van Kammen, W. B., Peters, J., Goetz, K., and Neylan, T. 1988. *Neuropsychopharmacology* **1**: 265–271.
- Wible, C. G., Shenton, M. E., Hokama, H., Kikinis, R., Jolesz, F. A., Metcalf, D., and McCarley, R. W. 1995. Prefrontal cortex and schizophrenia. A quantitative magnetic resonance imaging study. *Arch. Gen. Psychiatry* **52**: 279–288.
- Williams, A. O., Reveley, M. A., Kolakowska, T., Ardern, M., and Mandelbrote, B. M. 1985. Schizophrenia with good and poor outcome. II. Cerebral ventricular size and its clinical significance. *Br. J. Psychiatry* **146**: 239–246.
- Williamson, P., Pelz, D., Merskey, H., Morrison, S., and Conlon, P. 1991. Correlation of negative symptoms in schizophrenia with frontal lobe parameters on magnetic resonance imaging. *Br. J. Psychiatry* **159**: 130–134.
- Wright, I. C., McGuire, P. K., Poline, J. B., Travere, J. M., Murray, R. M., Frith, C. D., Frackowiak, R. S., and Friston, K. J. 1995. A voxel-based method for the statistical analysis of gray and white matter density applied to schizophrenia. *NeuroImage* **2**: 244–252.
- Wright, I. C., Sharma, T., Ellison, Z. R., McGuire, P. K., Friston, K. J., Brammer, M. J., Murray, R. M., and Bullmore, E. T. 1999. Supra-regional brain systems and the neuropathology of schizophrenia. *Cereb. Cortex* **9**: 366–378.
- Zipursky, R. B., Lim, K. O., Sullivan, E. V., Brown, B. W., and Pfefferbaum, A. 1992. Widespread cerebral gray matter volume deficits in schizophrenia. *Arch. Gen. Psychiatry* **49**: 195–205.